

Critical behavior in itinerant ferromagnet $\text{SrRu}_{1-x}\text{Ti}_x\text{O}_3$

Renu Gupta, Imtiaz Noor Bhatti, A. K. Pramanik

School of Physical Sciences, Jawaharlal Nehru University, New Delhi - 110067, India.

Abstract

SrRuO_3 presents a rare example of ferromagnetism among the $4d$ based oxides. While the nature of magnetic state in SrRuO_3 is mostly believed to be of itinerant type, recent studies suggest a coexistence of both itinerant and localized model of magnetism in this material. Here, we have investigated the evolution of magnetic state in doped $\text{SrRu}_{1-x}\text{Ti}_x\text{O}_3$ through studying the critical behavior using standard techniques such as, modified Arrott plot, Kouvel-Fisher plot and critical isotherm analysis across the magnetic transition temperature T_c . The substitution of nonmagnetic Ti^{4+} ($3d^0$) for Ru^{4+} ($4d^4$) would simply dilute the magnetic system apart from modifying the electron correlation effect and the density of states at Fermi level. Surprisingly, T_c does not change with x . Moreover, our analysis show the exponent β related to spontaneous magnetization increases while the exponents γ and δ related to initial inverse susceptibility and critical magnetization, respectively decrease with Ti substitution. The estimated exponents do not match with any established theoretical models for universality classes, however, the exponent obey the Widom relation and the scaling behavior. Interestingly, this particular evolution of exponents in present series has similarity with that in isoelectronic doped $\text{Sr}_{1-x}\text{Ca}_x\text{RuO}_3$. We believe that site dilution by Ti leads to formation magnetic clusters which causes this specific changes in critical exponents.

1. Introduction

The $4d$ based perovskite SrRuO_3 continues to attract large deal of scientific attention which includes both fundamental as well as technological interest. This material is commonly believed to be an itinerant type ferromagnet with transition temperature around 160 K, while offering a rare example of $4d$ based oxide having ferromagnetic (FM) ordering.[1, 2, 3, 4, 5, 6, 7] The itinerant nature of magnetic state is manifested in the fact that measured moment shows a lower value, $\sim 1.4 \mu_B/\text{f.u.}$ in magnetic field as high as 30 Tesla compared to expected spin-only value, $2 \mu_B/\text{f.u.}$ for $S = 1$. [2] Interestingly, a recent theoretical study [5] has predicted a coexistence both itinerant and localized nature of magnetism in SrRuO_3 which has also been experimentally discussed in our previous study. [6] Furthermore, debate continues about the nature of magnetism in SrRuO_3 . While the majority of studies report mean-field like magnetic state in SrRuO_3 , [7, 3, 8] there are several studies which imply 3D Heisenberg- or Ising-type spin interaction in this material. [9, 10, 11, 13] Interestingly, one recent

study shows that linearity in Arrott plot (signature for mean-field model) in SrRuO_3 is mainly realized due to continuous curvature evolution from $\text{Ca}_{0.5}\text{Sr}_{0.5}\text{RuO}_3$ to BaRuO_3 via SrRuO_3 as lattice distortions and spin-orbit coupling changes, and it is less likely due to itinerant type ferromagnetism in SrRuO_3 . [7] Similarly, influence of anisotropy on critical behavior where the exponent values change with crystal axis has also been shown for SrRuO_3 . [11, 12] This underlines the fact that even after large volume of study, the detail nature of magnetic state in SrRuO_3 is still debated.

There have been several attempts to understand the nature of magnetism using route of chemical substitution. The most prominent one is the isoelectronic substitution at Sr-site. The Ca^{2+} substitution in $\text{Sr}_{1-x}\text{Ca}_x\text{RuO}_3$ shows a total suppression of FM ordering at about 70% of doping concentration, a phenomenon which has been associated with the FM quantum phase transition (QPT) phenomenon. [3, 2] Band structure calculations show that substitution of Ca causes further distortion in RuO_6 octahedra and in Ru-O-Ru bond angle which effectively decreases the density of states at Fermi level $N(\epsilon_F)$, hence the necessary Stoner criterion for itinerant ferromagnet is no more satisfied. [4] The critical behavior in $\text{Sr}_{1-x}\text{Ca}_x\text{RuO}_3$ shows an interesting evolution where

Email address: akpramanik@mail.jnu.ac.in (A. K. Pramanik)

the exponent β increases, and both γ and δ decreases with Ca doping which has been attributed to effect of disorder arising from quantum fluctuation close to QPT point and phase segregation effect.[3, 7] On other hand, Ba^{2+} substitution in $\text{Sr}_{1-x}\text{Ba}_x\text{RuO}_3$ lowers the T_c down to about 60 K and the nature of magnetism is found to closely follow the 3D Heisenberg model.[14]

In present work, we have investigated the magnetic state in $\text{SrRu}_{1-x}\text{Ti}_x\text{O}_3$ by studying an evolution of critical behavior as the related critical exponents and critical temperature represent an intrinsic nature of magnetic behavior of a material. From structure wise, ionic radii of Ru^{4+} (0.62 Å) and Ti^{4+} (0.605 Å) closely match which implies this substitution will introduce minimum structural modification, hence the structural disorder induced modification in magnetic state is least expected. Rather, nonmagnetic Ti^{4+} would simply dilute the magnetic structure formed by transition metal and oxygen network. Further, substitution of Ti^{4+} ($3d^0$) for Ru^{4+} ($4d^4$) would oppositely tune the electron correlation U and $N(\epsilon_F)$ which will have wide ramification on Stoner criteria of itinerant FM i.e., $UN(\epsilon_F) > 1$. [15] Even, a large change of T_c has been observed with variation of $N(\epsilon_F)$ in ultra thin film of SrRuO_3 . [16] In fact, recently we have shown while effective magnetic moment and the Curie-Weiss temperature decreases in $\text{SrRu}_{1-x}\text{Ti}_x\text{O}_3$ with x , the FM transition temperature T_c appears to remain unchanged. [6] This unchanged behavior of T_c has been understood through an opposite tuning of U and $N(\epsilon_F)$ in picture of itinerant ferromagnet where the combined term $UN(\epsilon_F)$ effectively remains constant with Ti doping. In deed, photoemission spectroscopy measurements as well as band structure calculations have shown gradual increase of U and depletion of $N(\epsilon_F)$ with Ti substitution in SrRuO_3 . [17, 18] With Ti substitution, SrRuO_3 further develops Griffiths-phase like behavior which arises due to disorder coming from formation of magnetic clusters above T_c which has similarly been evidenced in $\text{Sr}_{1-x}\text{Ca}_x\text{RuO}_3$. [14] This present series of samples share some of the properties with isoelectronic doped $\text{Sr}_{1-x}\text{Ca}_x\text{RuO}_3$, therefore it would be interesting to understand the critical behavior in $\text{SrRu}_{1-x}\text{Ti}_x\text{O}_3$.

Here, we have studied the critical behavior in $\text{SrRu}_{1-x}\text{Ti}_x\text{O}_3$ series with $x = 0.0, 0.1, 0.3, 0.4, 0.5$ and 0.7 . We have estimated the critical exponents (β , γ and δ) and T_c following various independent methods such as, modified Arrott plot, Kouvel-Fisher method and critical isotherm analysis. The estimated exponent β for SrRuO_3 is close to the value for mean-field model (Table I). The exponents for doped materials do not match with the values theoretically predicted for different universality classes based on 3-dimensional magnetism.

The estimated exponents, however, obey the scaling law behavior and Widom relation which implies values are correct.

2. Experimental Details

Polycrystalline samples of series $\text{SrRu}_{1-x}\text{Ti}_x\text{O}_3$ with $x = 0.0, 0.1, 0.3, 0.4, 0.5$ and 0.7 are prepared by standard solid state method. The samples have been characterized by x-ray diffraction (XRD) and by Rietveld analysis of XRD data. All the samples are in single phase and without any noticeable chemical impurity. Details of sample preparation and characterization are given elsewhere. [6] Temperature (T) dependent magnetization (M) data have been collected with superconducting quantum interference device (SQUID) magnetometer by M/s Quantum Design. For critical analysis, magnetic field (H) dependent isotherms $M(H)$ have been collected at an interval of 1 K across T_c using vibrating sample magnetometer (VSM) by M/s Cryogenics Ltd. For proper stabilization of temperature, about 10 minute wait time has been given before recording each isotherm. The external applied magnetic field (H_a) has been corrected by the demagnetization effect to get the internal magnetic field $H_i [=H_a - N M(T, H_a)]$, where $M(T, H_a)$ is the measured magnetization and N in the demagnetization constant that has been calculated from physical dimensions of sample. [19] This calculated H_i has been used for critical exponent scaling analysis. The critical temperature and critical exponents are have been determined by commonly used techniques like modified Arrott plots (MAP), Kouvel-Fisher (KF) method and critical isotherm analysis.

3. Results and Discussions

3.1. Scaling Analysis

In case of second-order phase transition, the correlation length (ξ) among spins diverges at the magnetic phase transition temperature T_c following $\xi = \xi_0 |1 - (T/T_c)|^{-\nu}$ where ν is the exponent. Following this, scaling hypothesis predicts that spontaneous magnetization M_s below T_c , initial inverse susceptibility χ_0^{-1} above T_c and magnetization at T_c obey set of power law behavior with temperature as described below, [20]

$$M_s(T) = M_0(-t)^\beta, t < 0 \quad (1)$$

$$\chi_0^{-1}(T) = G(t)^\gamma, t > 0 \quad (2)$$

$$M = XH^{1/\delta}, t = 0 \quad (3)$$

where $t = (T - T_c)/T_c$ is the reduced temperature; M_0 , G and X are the critical amplitudes and β , γ and δ are the critical exponents. The scaling hypothesis further predicts magnetic equation of state which describes the relationship between $M(H, t)$, H and T in following manner,

$$M(H, t) = t^\beta f_\pm \left(\frac{H}{t^{\beta+\gamma}} \right) \quad (4)$$

where f_+ and f_- are the regular functions for $T > T_c$ and $T < T_c$, respectively. The Eq. 4 implies that for right values of critical temperature T_c and critical exponents β and γ , the scaled magnetization $m = t^{-\beta} M(H, t)$ plotted as a function of scaled field $h = t^{-(\beta+\gamma)} H$ would fall on two distinct curves for isotherms both above and below T_c .

3.2. DC Magnetization study

Fig. 1 shows dc magnetization data collected following field cooled (FC) protocol in magnetic field of 100 Oe for $\text{SrRu}_{1-x}\text{Ti}_x\text{O}_3$ series. Recently, we have shown an interesting evolution of magnetic behavior of $\text{SrRu}_{1-x}\text{Ti}_x\text{O}_3$ series.[6] For parent SrRuO_3 , we have observed the magnetic transition temperature $T_c \sim 163$ K which is in conformity with other studies.[1, 2, 3, 13] With site dilution through Ti substitution, while though the Curie-Weiss temperature (θ_p) and the magnetic moments decreases, interestingly the long-range magnetic ordering temperature T_c does not change. In scenario of itinerant ferromagnetism, we explained this constant nature of T_c through opposite tuning of density of states (DOS) and electronic correlation (U) with Ti substitution. As evident in main panel of Fig. 1, FC magnetization for all the samples show a sudden rise around 163 K which marks the T_c . The inset of Fig. 1 depicts ZFC magnetization data in a close temperature scale around T_c . As evident in inset figure, M_{ZFC} show peak around 163 K which does not change with x . Here, it can be mentioned that our critical analysis of $M_{FC}(T)$ data also shows a constant T_c in present $\text{SrRu}_{1-x}\text{Ti}_x\text{O}_3$ series. This analysis further shows critical exponent β related to magnetization for parent SrRuO_3 closely matches with that for mean field model, and the value of β increases with x . In following, we have undertaken detailed critical analysis to understand the effect of site dilution on critical behavior in $\text{SrRu}_{1-x}\text{Ti}_x\text{O}_3$ series.

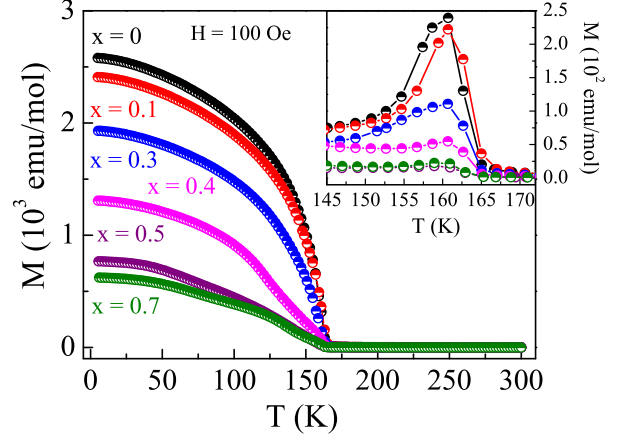


Figure 1: Temperature dependent field cooled magnetization data measured in presence of 100 Oe applied field have been shown for $\text{SrRu}_{1-x}\text{Ti}_x\text{O}_3$ series. The inset shows zero field cooled magnetization (100 Oe) in expanded temperature range close to T_c .

3.3. Arrott Plot

The Arrott plot offers an important tool to study the second-order magnetic phase transition and the critical behavior across second order PM-FM phase transition.[21] Arrott plot is about plotting of isothermal $M(H)$ data in form of M^2 vs H/M where for mean-field model with $\beta = 0.5$ and $\gamma = 1$, the isotherms form a set of parallel straight lines. In another sense, straight line behavior in high field regime in Arrott plot implies magnetic interaction is of mean-field type. Intercept due to straight line fitting in Arrott plot on M^2 and H/M axis directly gives spontaneous magnetization (M_s) and initial inverse susceptibility (χ_0^{-1}), respectively. Moreover, isotherm which passes through origin in Arrott plot marks the T_c as implies zero M_s . As discussed, for analysis of Arrott plot, a set of isotherms $M(H)$ is required across the T_c . Figs. 2a - 2f show isotherms (M vs H) plots) collected at different temperatures with temperature interval of $\Delta T = 1$ K across T_c for $\text{SrRu}_{1-x}\text{Ti}_x\text{O}_3$ series. The $M(H)$ plots for all the samples look like FM type where it shows downward curvature. Inset in each figure of Fig. 2 shows a derivative of magnetization (dM/dH) as a function of field for one representative temperature. Inset figures show a decreasing slope of $M(H)$ plot with field. This constitutes a typical signature of second-order PM to FM transition and justifies for following critical analysis.

Figs. 3a - 3f show Arrott plot, constructed from $M(H)$ isotherm data shown in Fig. 2 for $\text{SrRu}_{1-x}\text{Ti}_x\text{O}_3$ series. For parent SrRuO_3 , nature of magnetic state has mostly been shown by earlier studies to follow mean-field interaction model.[3] As discussed, for mean-field model

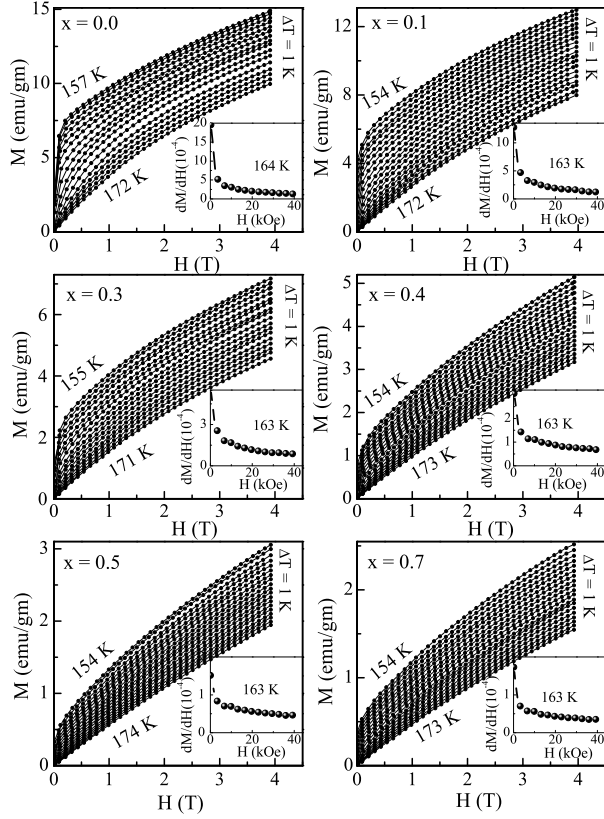


Figure 2: Field dependent isothermal magnetization data near to the transition temperature $\sim T_c$ are shown for $\text{SrRu}_{1-x}\text{Ti}_x\text{O}_3$ series with (a) $x = 0.0$ (b) $x = 0.1$ (c) $x = 0.3$ (d) $x = 0.4$ (e) $x = 0.5$ and (f) $x = 0.7$ composition. Inset of each figure shows magnetic-field derivative of magnetization (dM/dH) as a function of magnetic field for $M(H)$ plots taken at T_c for respective sample.

with critical exponents $\beta = 0.5$ and $\gamma = 1$, the Arrott plot should yield set of parallel straight lines. Arrott plot for SrRuO_3 in Fig. 3a show isotherms do not form straight lines even in high field regime, they are rather slightly curved in upward direction. This means critical exponents for SrRuO_3 do not exactly match with mean-field model but they are close to the mean-field values. Fig. 3 further shows with increasing x , nonlinearity in Arrott plot increases which suggests nature of magnetic interaction moves away from mean-field model as Ti is introduced in SrRuO_3 . As we do not obtain parallel straight lines with mean-field exponents, the analysis in Fig. 3 suggests new set of exponents need to be identified for straight line behavior.

To determine the critical exponents and temperature correctly for the present series of samples, we have employed modified Arrott plot (MAP) which is generalized form of Arrott plot and is based on Arrott-Noakes equa-

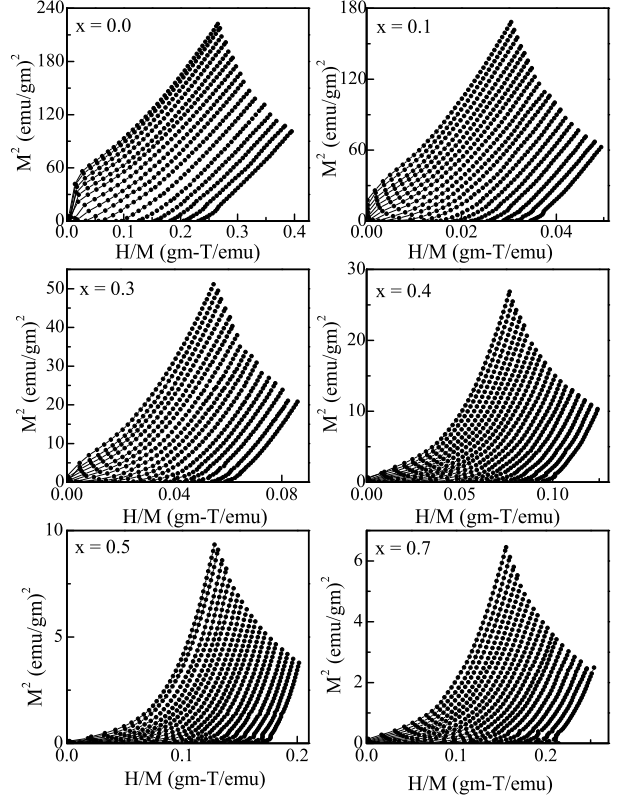


Figure 3: Isotherms in Fig. 2 are plotted in form of Arrott plot (M^2 vs H/M) for $\text{SrRu}_{1-x}\text{Ti}_x\text{O}_3$ series with (a) $x = 0.0$ (b) $x = 0.1$ (c) $x = 0.3$ (d) $x = 0.4$ (e) $x = 0.5$ and (f) $x = 0.7$.

tion of state given as,[22]

$$\left(\frac{H}{M}\right)^{1/\gamma} = a \frac{T - T_c}{T} + bM^{1/\beta} \quad (5)$$

where a and b are the constant. It is obvious that for $\beta = 0.5$ and $\gamma = 1$, Eq. 5 recovers Arrott plot discussed above. Following MAP, isotherms are plotted in form of $M^{1/\beta}$ vs $(H/M)^{1/\gamma}$. Here, we note that we have also tried to form MAP with the exponents β and γ which are theoretically predicted for 3-dimensional models such as, 3D Heisenberg, 3D Ising, 3D XY models, etc. (Table I) but remain unsuccessful in getting parallel straight lines. As the exponents $\beta = 0.5$ and $\gamma = 1$ do not yield straight lines in Fig. 3, we have tuned the exponents β and γ to obtain parallel straight lines. However, tuning of these parameters is not a straightforward job as two unknown parameters are involved and this often leads to erroneous results. Here, we have adopted an iterative method where we initially tuned β and γ in Eq. 5 to get apparently good parallel straight lines in modified Arrott plot.[23, 24] Then, temperature dependent

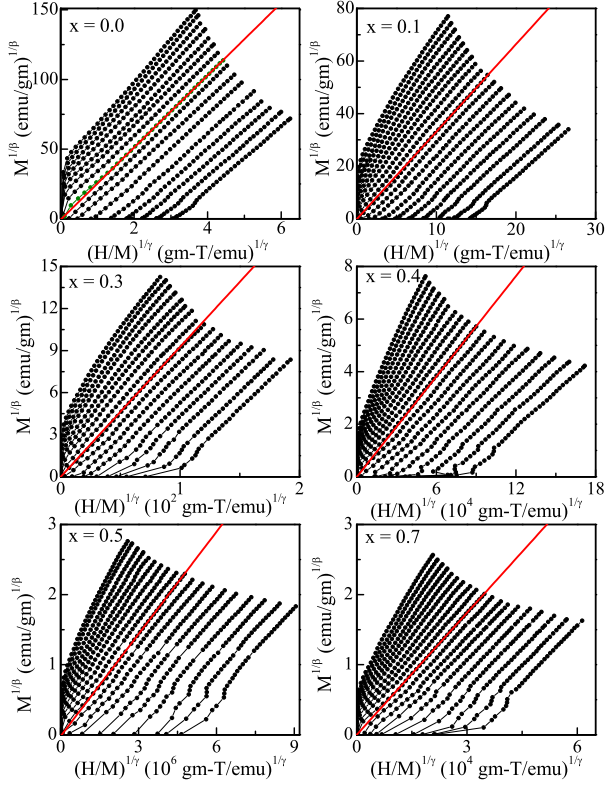


Figure 4: Modified Arrott plot, $M^{1/\beta}$ vs $(H/M)^{1/\gamma}$, constructed out of $M(H)$ data in Fig. 2 are shown for SrRu_{1-x}Ti_xO₃ series with (a) $x = 0.0$ (b) $x = 0.1$ (c) $x = 0.3$ (d) $x = 0.4$ (e) $x = 0.5$ and (f) $x = 0.7$. The solid red line in each figure is due to straight line fitting of modified Arrott plot related to isotherm which passes through origin.

$M_s(T)$ and $\chi_0^{-1}(T)$ have been obtained from intercept of straight fitting in MAP on $M^{1/\beta}$ and $(H/M)^{1/\gamma}$ axis, respectively. The T_c has been identified as the temperature whose $M(H)$ isotherm passes through origin in MAP. These $M_s(T)$, $\chi_0^{-1}(T)$ and T_c are then used in Eq. 1 and 2 to obtain new set of β and γ . These new values of β and γ have been used to construct similar MAP. This process has been continued till a convergence in values of critical exponents β and γ and critical temperature T_c is obtained. Figs. 4a - 4f show the MAP of isotherms shown in Figs. 2a - 2f in vicinity of T_c for all the samples. For parent SrRuO₃, we find that $\beta = 0.54$ and $\gamma = 0.75$ yield parallel straight lines where isotherm at 164 K passes through origin marking the T_c of this material (Fig. 4a). The same iterative method has been followed for all the samples. Figs. 4a - 4f show the MAP for all the samples in present series where reasonably good parallel straight lines have been formed in high field regime with proper choice of exponents β and γ .

The finally obtained M_s and χ_0^{-1} have been shown

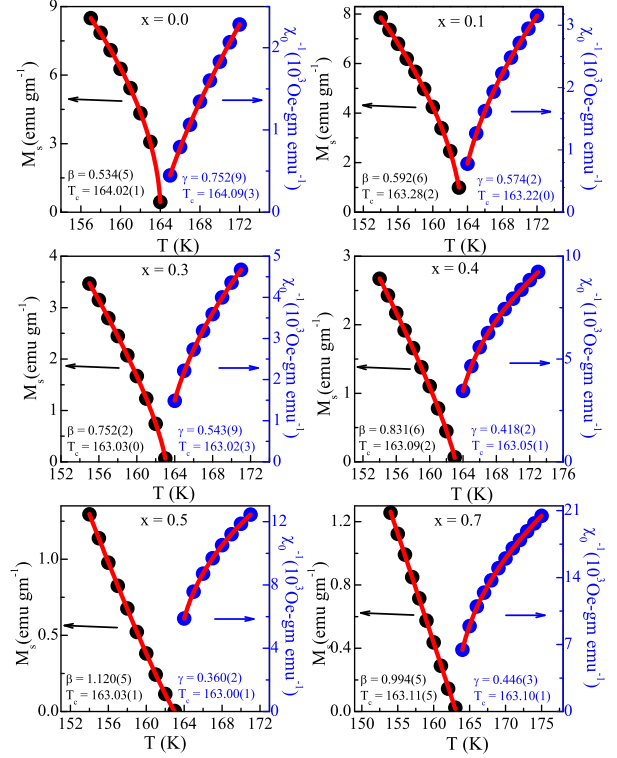


Figure 5: Temperature dependent spontaneous magnetization M_s (left axis) and initial inverse susceptibility $\chi_0^{-1}(T)$ (right axis) as estimated from modified Arrott plots in Fig. 4 are shown for SrRu_{1-x}Ti_xO₃ series with (a) $x = 0.0$ (b) $x = 0.1$ (c) $x = 0.3$ (d) $x = 0.4$ (e) $x = 0.5$ and (f) $x = 0.7$. The solid red lines are due to fitting with power law behavior as stated in Eq. 1 and 2.

as a function of temperature in Figs. 5a - 5f, showing M_s cease to exist once temperature approaches T_c . The $M_s(T)$ and $\chi_0(T)$ data in Figs. 5a - 5f have been fitted with Eqs. 1 and 2, respectively for all the compositions. The exponents β and γ and respective T_c following MAP method. Table I shows the exponents β and γ and respective T_c following MAP method. From fitting of $M_s(T)$ with Eq. 1 we obtain $\beta = 0.534(5)$ and $T_c = 164.02(1)$ K and from fitting of $\chi_0^{-1}(T)$ with Eq. 2 we get $\gamma = 0.752(9)$ and $T_c = 164.09(3)$ K. These values of β , γ and T_c are significantly close to the values obtained using MAP in Fig. 4 which underlines the correctness of our iterative method. The T_c values obtained from both $M_s(T)$ and $\chi_0(T)$ in MAP show consistent behavior for whole series. For SrRuO₃, obtained $T_c \sim 164$ K matches well with the reported values. Remarkably, T_c remains almost constant with Ti substitution in present series which substantiates our earlier results. [6] The obtained exponents β and γ do not exactly match with the values theoretically predicted for three dimensional

systems (Table I), however, values look closer to mean-field model for $x = 0.0$ material.

3.4. Kouvel-Fisher plot

Alternatively, critical exponents β and γ and the critical temperature T_c have been determined using more accurate Kouvel-Fisher (KF) method where the M_s and χ_0^{-1} are analyzed using Eqs. 6 and 7, respectively.[25] The KF plot for whole series of samples has been shown in Figs. 6a - 6f where $M_s(T)[dM_s(T)/dT]^{-1}$ vs T and $\chi_0^{-1}(T)[d\chi_0^{-1}(T)/dT]^{-1}$ vs T are plotted. According to KF method (Eq. 6 and 7), these plots would result in straight line behavior where the respective slope would give $1/\beta$ and $1/\gamma$. In addition, T_c can be obtained directly and independently as the intercept on temperature axis would give T_c . In deed, Fig. 6 shows KF plot forms reasonable straight lines for all the samples which confirms the correctness of KF analysis. For SrRuO₃, we obtain exponents $\beta = 0.542(8)$ and $T_c = 164.02(3)$, and $\gamma = 0.753(6)$ and $T_c = 164.08(3)$. These values of β , γ and T_c obtained from KF plot are given in Table I for all the compositions. It is remarkable that values of exponents and T_c obtained from KF plots match closely with those obtained from MAP analysis. With Ti substitution, while β increases away from the mean-field value and, on other hand, the γ decreases. Nonetheless, agreement between values obtained from two independent MAP and KF method is quite remarkable indicating obtained values are correct.

$$M_s(T)[dM_s(T)/dT]^{-1} = \frac{T - T_c}{\beta} \quad (6)$$

$$\chi_0^{-1}(T)[d\chi_0^{-1}(T)/dT]^{-1} = \frac{T - T_c}{\gamma} \quad (7)$$

3.5. Critical isotherm plot

Scaling analysis predicts that variation of $M(H)$ at T_c (critical isotherm) follows a power-law behavior involving exponent δ (Eq. 3). Critical isotherms are already identified from MAP in Fig. 4. The main panel of Figs. 7a - 7f shows critical isotherms $M(H, T_c)$ for all samples in present series. The inset of Figs. 7a - 7f show same plot in \log_{10} - \log_{10} scale. Following Eq. 3, slope due to straight line fitting in $\log M$ vs $\log H$ plot would give $1/\delta$. The inset plots show reasonably linear behavior, and the exponent δ calculated from slope is given in Table I as critical isotherm method. Again, obtain δ does not match with the theoretical values predicted

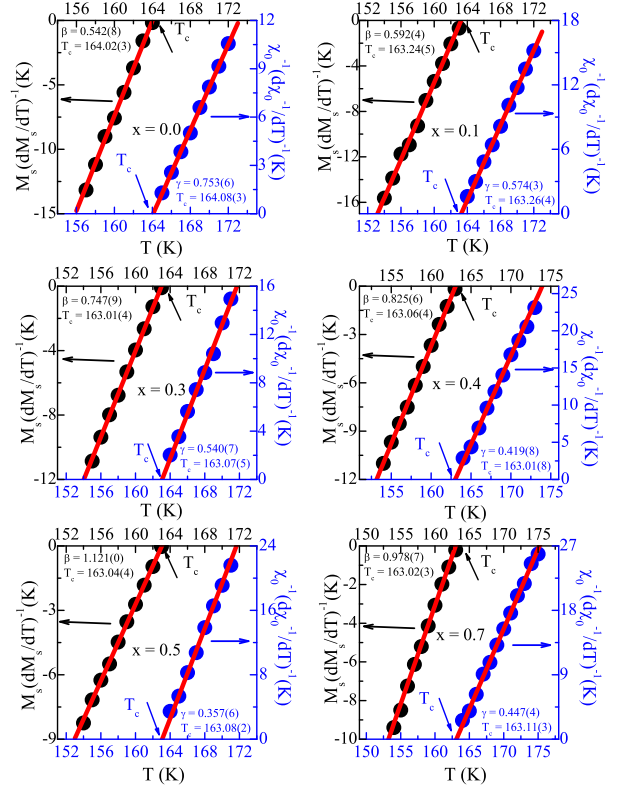


Figure 6: Kouvel-Fisher plots for spontaneous magnetization (Eq. 6) on left axis and for initial inverse susceptibility (Eq. 7) on right have been shown for SrRu_{1-x}Ti_xO₃ series with (a) $x = 0.0$ (b) $x = 0.1$ (c) $x = 0.3$ (d) $x = 0.4$ (e) $x = 0.5$ and (f) $x = 0.7$. The solid straight lines are the linear fits following Eq. 6 and 7.

for 3D based different universality classes as mentioned in Table I. To crosscheck the consistency of the estimated exponents, we have used Widom scaling relation where the critical exponents β , γ and δ obey following relation,[27]

$$\delta = 1 + \frac{\gamma}{\beta} \quad (8)$$

Eq. 8 indirectly gives exponent δ using the values of exponents γ and β . The δ has been calculated following Eq. 8 using β and γ values which are estimated from both MAP and KF plot methods. Table I shows exponent δ where the values represent both obtained from analysis of critical isotherm as well as calculated from using Eq. 8. For SrRuO₃, we obtain $\delta = 2.389(3)$ following critical isotherm analysis (Fig. 7) and 2.408(2) and 2.389(2) from MAP and KF plot using Eq. 8. Both the estimated and calculated values match well. With Ti substitution, δ continuously decreases till $x = 0.5$ and

then shows an increased value for $x = 0.7$. It is remarkable that values of δ obtained from two distinct process agree reasonably for all the materials which emphasizes that values of exponents β , γ , δ and temperature T_c are estimated quite accurately.

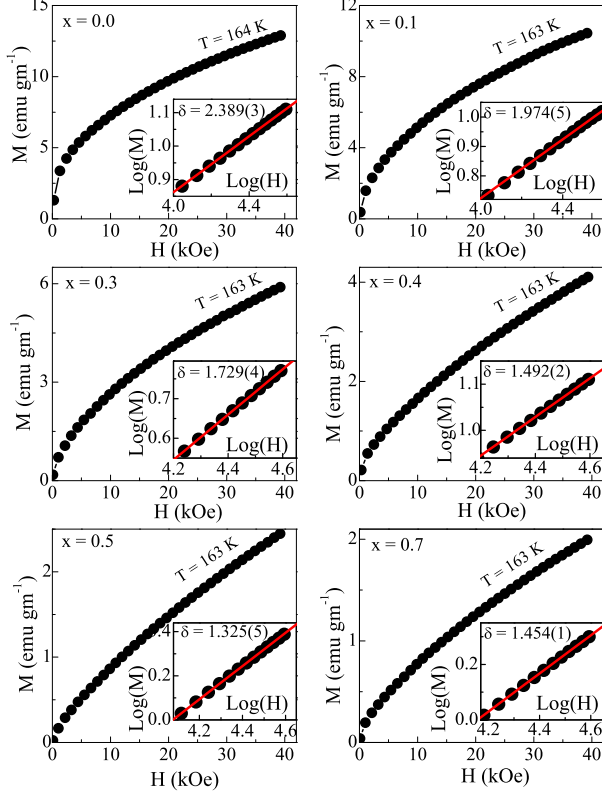


Figure 7: The $M(H)$ isotherm at T_c has been shown for $\text{SrRu}_{1-x}\text{Ti}_x\text{O}_3$ series with (a) $x = 0.0$ (b) $x = 0.1$ (c) $x = 0.3$ (d) $x = 0.4$ (e) $x = 0.5$ and (f) $x = 0.7$. The inset shows same $M(H)$ data in \log_{10} - \log_{10} scale for respective samples and the solid line is due to linear fit of the data.

3.6. Scaling analysis

So far we have seen that critical exponents in present series do not exactly match with any established theoretical models for classical spin interaction. However, the exponents and T_c determined using different independent methods such as, modified Arrott plot, Kouvel-Fisher plot and critical isotherm analysis agree very closely (Table I). Moreover, exponents follow Widom relation. We have further tested the consistency and accuracy of exponents as well as T_c using a scaling analysis (Eq. 4). This analysis suggests plotting of magnetic isotherm $M(H)$ data in form of $M|t|^{-\beta}$ vs $H|t|^{-(\gamma+\beta)}$

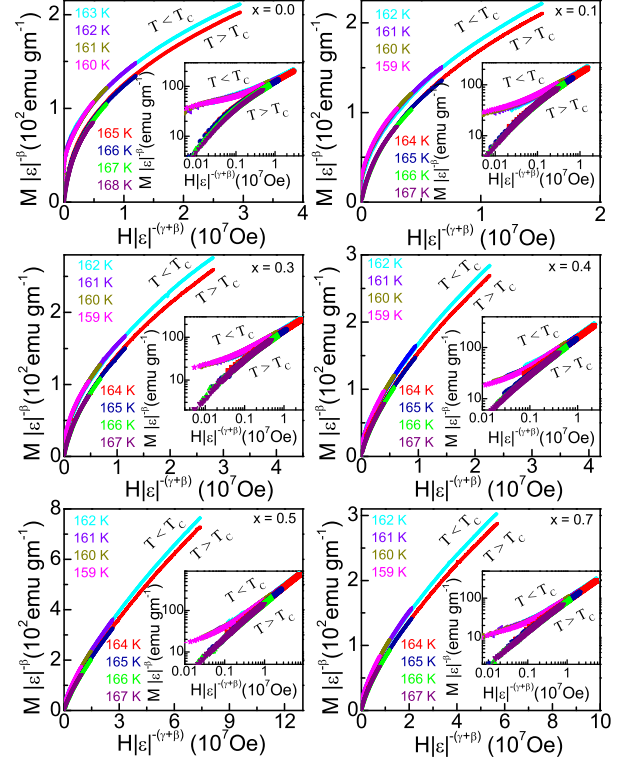


Figure 8: Renormalized magnetization $M|t|^{-\beta}$ has been plotted as a function of renormalized field $H|t|^{-(\gamma+\beta)}$ for isotherms both below and above T_c . Data are shown for $\text{SrRu}_{1-x}\text{Ti}_x\text{O}_3$ series with (a) $x = 0.0$ (b) $x = 0.1$ (c) $x = 0.3$ (d) $x = 0.4$ (e) $x = 0.5$ and (f) $x = 0.7$. Inset shows same plot in \log_{10} - \log_{10} scale. Renormalized magnetization is merged into single line with renormalized field for isotherms both below and above T_c .

where the isotherms both below and above T_c are scaled into a separate line for correct values of critical exponents and T_c . This rather constitutes a rigorous test to examine the consistency and accuracy of exponents as well as T_c . Scaling plots are shown in Figs. 8a - 8f for this present series where four scaled isotherms both below and above of respective T_c are plotted following Eq. 4. As seen in Fig. 8, isotherms both below and above T_c are nicely scaled into a line. The same plot are shown in \log_{10} - \log_{10} scale in inset of Fig. 8 for better presentation which also shows a nice scaling of isotherm data. This reconfirms that estimated exponents (β , γ and δ) as well as T_c in Table I for all the samples in this series are accurate and consistent.

3.7. Evolution of exponents in $\text{SrRu}_{1-x}\text{Ti}_x\text{O}_3$

Our experimental data analysis show critical exponent β for SrRuO_3 is close to the mean-field value 0.5, however, exponents γ and δ show the values lower than

¹Calculated following Eq. 8

Table 1: Table shows the values of critical exponents β , γ and δ determined using different independent methods such as modifier Arrott plot (MAP), Kouvel-Fisher (KF) plot and critical isotherm analysis for $\text{SrRu}_{1-x}\text{Ti}_x\text{O}_3$ series. The values of exponents calculated theoretically following different spin interaction models are also given for comparison.

Composition	Ref.	Method	β	$T_c(M_s)$	γ	$T_c(\chi_0)$	δ
SrRuO_3	This work	MAP	0.534(5)	164.02(1)	0.752(9)	164.09(3)	2.408(2) ¹
		KF Method	0.542(8)	164.02(3)	0.753(6)	164.08(3)	2.389(2) ¹
		Critical Isotherm					2.389(3)
$\text{SrRu}_{0.9}\text{Ti}_{0.1}\text{O}_3$	This work	MAP	0.592(6)	163.28(6)	0.574(2)	163.22(0)	1.969(5) ¹
		KF Method	0.592(4)	163.24(5)	0.574(3)	163.26(4)	1.969(5) ¹
		Critical Isotherm					1.974(5)
$\text{SrRu}_{0.7}\text{Ti}_{0.3}\text{O}_3$	This work	MAP	0.752(2)	163.03(2)	0.543(9)	163.02(3)	1.722(0) ¹
		KF Method	0.747(9)	163.01(4)	0.540(7)	163.07(3)	1.722(8) ¹
		Critical Isotherm					1.729(4)
$\text{SrRu}_{0.6}\text{Ti}_{0.4}\text{O}_3$	This work	MAP	0.831(6)	163.09(2)	0.418(2)	163.05(1)	1.503(0) ¹
		KF Method	0.825(6)	163.06(4)	0.419(8)	163.01(8)	1.507(8) ¹
		Critical Isotherm					1.492(2)
$\text{SrRu}_{0.5}\text{Ti}_{0.5}\text{O}_3$	This work	MAP	1.120(5)	163.03(1)	0.360(2)	163.00(1)	1.321(4) ¹
		KF Method	1.121(0)	163.04(4)	0.357(6)	163.08(2)	1.318(4) ¹
		Critical Isotherm					1.325(5)
$\text{SrRu}_{0.3}\text{Ti}_{0.7}\text{O}_3$	This work	MAP	0.994(5)	163.11(5)	0.446(3)	163.10(1)	1.448(6) ¹
		KF Method	0.978(7)	163.02(3)	0.447(4)	163.11(3)	1.457(0) ¹
		Critical Isotherm					1.454(1)
Mean-field Model	[26]	Theory	0.5		1.0		3.0
3D Heisenberg Model	[26]	Theory	0.365		1.386		4.8
3D Ising Model	[26]	Theory	0.325		1.241		4.82

those for mean-field model i.e., 1.0 and 3.0, respectively (see Table I). For SrRuO_3 , we obtain $T_c \sim 164$ K which is very consistent with reported values for this material,[1, 2, 3, 7, 13] even this T_c is one of the highest value obtained for this material. Our critical analysis interestingly show that substitution of Ti has very little influence on T_c of SrRuO_3 as we find T_c remains almost unchanged. This is in conformity with our earlier study where we have explained this constant behavior of T_c in $\text{SrRu}_{1-x}\text{Ti}_x\text{O}_3$ considering opposite change of electron correlation U and density of states $N(\epsilon_F)$ that maintains T_c in picture of itinerant ferromagnet.

Nonetheless, critical exponents show an unusual evolution where β increases and both γ and δ decreases with x (see Table I). In Fig. 9, we have shown an evolution of exponents β , γ and δ with Ti (x) normalized by respective values for SrRuO_3 ($x = 0$). The figure shows that β continuously increases and γ , δ decreases till $x = 0.5$, though for $x = 0.7$ the values appear to show a reverse turn which may be related to metal-to-insulator transition around $x \sim 0.4$ in $\text{SrRu}_{1-x}\text{Ti}_x\text{O}_3$ series.[28] Here, we mention that critical exponents and T_c are obtained using different independent techniques namely, MAF, KF plot and critical isotherm analysis and they

nicely agree. It can be noted that determined exponents and T_c fairly obey the scaling law behavior (Fig. 8) for all the samples. Moreover, the Widom relation (Eq. 8), which demonstrates relation among the critical exponents is nicely followed for entire range of Ti doping (Table I). These attest to the fact that determined exponents and T_c are consistent and correct with experimental accuracy. These exponents show a steady variation and deviates from mean-field behavior with increasing x . However, the exponent values do not match with the predicted values for different known universality class models, also those can not be explained with theoretical models available at hands for spin exchange interaction. Note, that similar kind of evolution of critical exponents (β , γ and δ) has been evidenced in $\text{Sr}_{1-x}\text{Ca}_x\text{RuO}_3$, however, prominent difference is that T_c decreases to zero around 70% of Ca doping resulting in quantum phase transition whereas T_c remains almost unchanged in present series.[3, 7, 6] In case of $\text{Sr}_{1-x}\text{Ca}_x\text{RuO}_3$, this particular evolution of exponents has been attributed to crossover from mean-field like behavior to disorder-induced strong coupling regime arising from quantum fluctuations near quantum phase transition point by Fuchs *et al.*[3] An another study reports

that following of Arrott plot (signature of mean-field model) in SrRuO_3 may not be associated with itinerant model of magnetism, rather this arises due to continuous curvature evolution from $\text{Sr}_{0.5}\text{Ca}_{0.5}\text{RuO}_3$ to SrRuO_3 to BaRuO_3 as induced by changes in lattice distortion and spin-orbit coupling effect.[7] These changes are responsible for band narrowing in $\text{Sr}_{1-x}\text{Ca}_x\text{RuO}_3$ which leads to phase segregation between strongly and weakly correlated phases, hence exponents evolve accordingly. Here, it can be further noted that in heavy fermion compound $\text{URu}_{1-x}\text{Re}_x\text{Si}_2$, while though exponent β remains constant but the exponents γ and $(\delta - 1)$ decreases to zero as the QPT is approached with decreasing Re substitution around 15%.[29]

While though the magnetic moment and the Curie-Weiss temperature decreases in $\text{SrRu}_{1-x}\text{Ti}_x\text{O}_3$ but the ferromagnetic T_c does not modify unlike in case of $\text{Sr}_{1-x}\text{Ca}_x\text{RuO}_3$. [3, 14, 7] Moreover, minimum structural modification due to almost matching ionic size between Ru^{4+} and Ti^{4+} in present $\text{SrRu}_{1-x}\text{Ti}_x\text{O}_3$ series would unlikely cause this peculiar changes in exponents. This system, however, does not convert into first order type PM-FM transition with Ti as seen from decreasing slope in $M(H)$ plot in Fig. 2. Nonetheless, this unusual change in exponents (β , γ and δ) is quite intriguing as their values substantially depart from mean-field values ($\beta = 0.5$, $\gamma = 1.0$ and $\delta = 3.0$), and also from the values typically realized for classical ferromagnetic systems ($\beta < 0.5$, $\gamma > 1.0$ and $\delta > 3.0$). We believe that Ti substituted at Ru-site dilutes the magnetic exchange path, and at higher doping concentration of Ti the system develops into small-size magnetic clusters which is manifested through Griffiths phase like behavior, as reported in our earlier study.[6] This has another striking similarity with $\text{Sr}_{1-x}\text{Ca}_x\text{RuO}_3$ which also exhibits GP like behavior with progressive doping of Ca.[14, 7] The disorder is prerequisite for the GP property which is provided by structural distortion in $\text{Sr}_{1-x}\text{Ca}_x\text{RuO}_3$ whereas site dilution achieved by Ti substitution acts as source of disorder in present $\text{SrRu}_{1-x}\text{Ti}_x\text{O}_3$. Henceforth, we speculate that effect of disorder realized from both Ti as well as magnetic clusters can provide possible explanation for this unusual change in critical exponents where β increases and both γ and δ decreases. The value of γ lower than unity in SrRuO_3 suggests parent $x = 0$ sample has some disorder or phase inhomogeneity above T_c . This effect of these changes in exponents is quite evident in Fig. 1 where the PM-FM phase transition broadens with progressive Ti substitution. In fact, a recent optical spectroscopy study has shown the temperature dependence of optical conductivity spectra indicates itinerant-type FM in SrRuO_3 . [30] This study

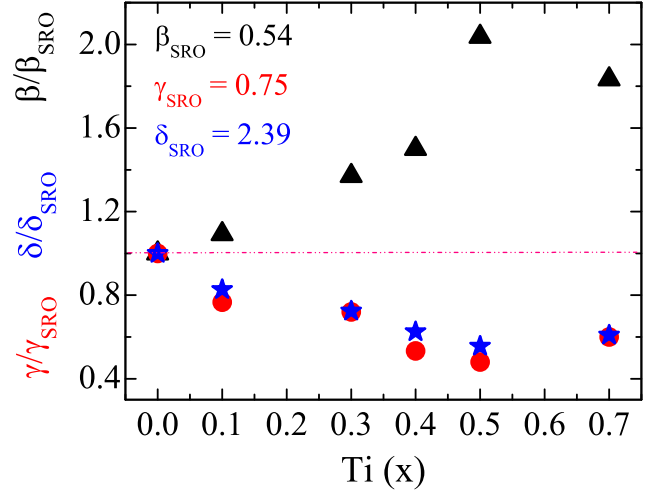


Figure 9: The critical exponents scaled by its values for $x = 0.0$ compound are shown as a function of composition (x) for $\text{SrRu}_{1-x}\text{Ti}_x\text{O}_3$ series.

further demonstrates non-vanishing local spin moment (sub-micron size) at $T > T_c$ (PM state) originating from local-band exchange splitting which is explained with fluctuating local band theory. However, the net moment is realized to be zero due to spatial and temporal fluctuations of local bands. This needs to be understood whether this renders a constant T_c in present $\text{SrRu}_{1-x}\text{Ti}_x\text{O}_3$ series.

4. Conclusion

In summary, we have studied the critical behavior in perovskite based $\text{SrRu}_{1-x}\text{Ti}_x\text{O}_3$ as a function of Ti substitution using the standard methods such as, modified Arrott plot, Kouvel-Fisher plot and critical isotherm analysis. We have estimated critical exponents β , γ and δ where β increases and both γ and δ decreases with Ti substitution. The transition temperature T_c , however, remains almost unchanged with site dilution by Ti doping. The estimated exponents do not match with the values of any universality classes known for spin interaction models. Nonetheless, the exponents nicely obey the Widom relation as well as scaling behavior which attest to the fact that estimated exponents and T_c are consistent and accurate. The evolution of exponents of similar nature has been observed in isoelectronic doped $\text{Sr}_{1-x}\text{Ca}_x\text{RuO}_3$. This specific change of exponents is likely caused by disorders arising from magnetic clusters which originates due to site dilution with Ti substitution. The evolution of Griffiths phase like behavior in present series as evidenced in our earlier study substan-

tiates the formation of magnetic clusters and its influences on the magnetic behavior.

5. Acknowledgment

We acknowledge Advanced Instrumentation Research Facility (AIRF), JNU for magnetization measurements. We thank Mr. Saroj Jha for the help during the measurements. RG and INB acknowledge the financial support from UGC, India for BSR fellowship and from CSIR, India for SRF Fellowship, respectively.

References

- [1] P. B. Allen, H. Berger, O. Chauvet, L. Forro, T. Jarlborg, A. Junod, B. Revaz and G. Santi, Phys. Rev. B **53** (1996), 4393
- [2] G. Cao, S. McCall, M. Shepard, J. E. Crow and R. P. Guertin, Phys. Rev. B **56** (1997), 321
- [3] D. Fuchs, M. Wissinger, J. Schmalian, C. L. Huang, R. Fromknecht, R. Schneider and H. V. Lohneysen, Phys. Rev. B **89** (2014), 174405
- [4] I. I. Mazin and D. J. Singh, Phys. Rev. B **56** (1997), 2556
- [5] M. Kim and B. I. Min, Phys. Rev. B **91** (2015), 205116
- [6] R. Gupta and A. K. Pramanik, J. Phys.: Condens. Matter **29** (2017), 115801
- [7] J.-G. Cheng, J.-S. Zhou, J. B. Goodenough, and C.-Q. Jin, Phys. Rev. B **85** (2012), 184430
- [8] D. Kim, B. L. Zink, F. Hellman, S. McCall, G. Cao, and J. E. Crow, Phys. Rev. B **67** (2003), 100406
- [9] R. Palai, H. Huhtinen, J. F. Scott, and R. S. Katiyar, Phys. Rev. B **79** (2009), 104413
- [10] Y. Kats, L. Klein, J. W. Reiner, T. H. Geballe, M. R. Beasley, and A. Kapitulnik, Phys. Rev. B **63** (2001), 054435
- [11] L. Klein, J. S. Dodge, C. H. Ahn, J. W. Reiner, L. Mieville, T. H. Geballe, M. R. Beasley and A. Kapitulnik, J. Phys.: Condens. Matter **8** (1996), 10111
- [12] L. M. Wang, H. E. Horng and H. C. Yang, Phys. Rev. B **70** (2004), 014433
- [13] C. Sow, D. Samal, P. S. Anil Kumar, A. K. Bera and S. M. Yusuf, Phys. Rev. B **85** (2012), 224426
- [14] C. -Q. Jin, J. -S. Zhou, J. B. Goodenough, Q. Q. Liu, J. G. Zhao, L. X. Yang, Y. Yu, R. C. Yu, T. Katsura, A. Shatskiy and E. Ito, Proc. Natl Acad. Sci. USA, **105** (2008), 7115
- [15] E. C. Stoner, Proc. R. Sco. London, **169** (1939), 339
- [16] Y. J. Chang, C. H. Kim, S. H. Phark, Y. S. Kim, J. Yu and T. W. Noh, Phys. Rev. Lett. **103** (2009), 057201
- [17] J. Kim, J.-Y. Kim, B.-G. Park and S.-J. Oh, Phys. Rev. B **73** (2006), 235109
- [18] P.-A. Lin, H.-T. Jeng, and C.-S. Hsue Phys. Rev. B **77** (2008), 085118
- [19] J. A. Osborn, Phys. Rev. **67** (1945), 351
- [20] H. E. Stanley, *Introduction to Phase Transitions and Critical Phenomena* (Oxford University Press, London, 1971).
- [21] A. Arrott, Phys. Rev. **108** (1957), 1394
- [22] A. Arrott and J. E. Noakes, Phys. Rev. Lett. **19** (1967), 786
- [23] A. K. Pramanik and A. Banejee, Phys. Rev. B **79** (2009), 204426
- [24] Imtiaz Noor Bhatti and A. K. Pramanik, J. Magn. Magn. Mater. **422** (2017), 141
- [25] J. S. Kouvel, and M. E. Fisher, Phys. Rev. **136** (1964), A1626
- [26] S. N. Kaul, J. Magn. Magn. Mater. **53** (1985), 5
- [27] B. Widom, J. Chem. Phys. **43**, 3898 (1965); **41** (1964), 1633
- [28] K. W. Kim, J. S. Lee, and T. W. Noh, S. R. Lee and K. Char, Phys. Rev. **71** (2005), 125104
- [29] N. P. Butch and M. B. Maple, Phys. Rev. Lett. **103** (2009), 076404
- [30] D. W. Jeong, H. C. Choi, C. H. Kim, S. H. Chang, C. H. Sohn, H. J. Park, T. D. Kang, D.-Y. Cho, S. H. Baek, C. B. Eom, J. H. Shim, J. Yu, K. W. Kim, S. J. Moon, and T. W. Noh, Phys. Rev. Lett. **110** (2013), 247202